Analytical Prediction of the Incremental Inductance of the Permanent Magnet Synchronous Motors

Shyh-Jier Wang and Shir-Kuan Lin

***Abstract*—An analytical method for calculating the incremental line inductance of a permanent-magnet synchronous motor is proposed in this paper. First, the incremental inductance is simplified as a linear combination of the slot inductance and the air-gap inductance, which are both estimated by the equivalent magnetic circuits. The reluctance of the rotor back irons and the stator back irons are ignored when the slot inductance is calculated. However, for the calculation of the air-gap inductance, the iron saturations and the perturbations of the permanent magnet are considered. The proposed method is verified by a finite-element method.**

***Index Terms*—Analytical method, finite-element method, incremental inductance, iron saturation, permanent magnet synchronous.**

I. Introduction

IT IS KNOWN that the accurate calculation of the winding inductance is essential for the design of a permanent-magnet synchronous motor (PMSM). Several works have been presented to deal with the calculation of the winding inductance of a PMSM. The two-dimensional (2-D) analytical method proposed by Zhu [1] ignored the reluctance of the rotor back irons and the stator irons, although it was simple. A numerical method based on the finite-element method (FEM) was presented by Lowther [2]. He ignored the perturbations of the permanent magnet (PM). On the other hand, Demerdash [3] and Gyimesi [4] proposed FEM methods to deal with the so-called incremental inductance. These methods took into account the effects of the iron saturation, so that the variation of the incremental inductance with the rotor position and the winding current can be predicted. However, little attention has been paid to the development of an analytical method for the computation of the incremental inductance of a PMSM.

This paper is aimed at the development of an analytical method for the incremental inductance of a PMSM, which can enormously reduce computations in comparison with FEM.

II. Main Result

It is known that the line inductance of a PMSM, denoted by L_t, can be described as follows [5]: $L_t = L_{\rm eq} + L_{\rm end}$ where $L_{\rm eq}$ is the 2-D equivalent inductance, $L_{\rm end}$ is the end-turn inductance of windings. $L_{\rm end}$ is brought by three-dimensional (3-D) magnetic flux in a PMSM, and is usually much less than $L_{\rm eq}$.

Manuscript received October 15, 2003. This paper was supported in part by the National Science Council of Taiwan under Grant NSC 92-2213-E-009-057.

The authors are with the Department of Electrical and Control Engineering, National Chiao Tung University, Hsinchu 300, Taiwan, R.O.C. (e-mail: sjwang@itri.org.tw; sklin@cc.nctu.edu.tw).

Digital Object Identifier 10.1109/TMAG.2004.830629

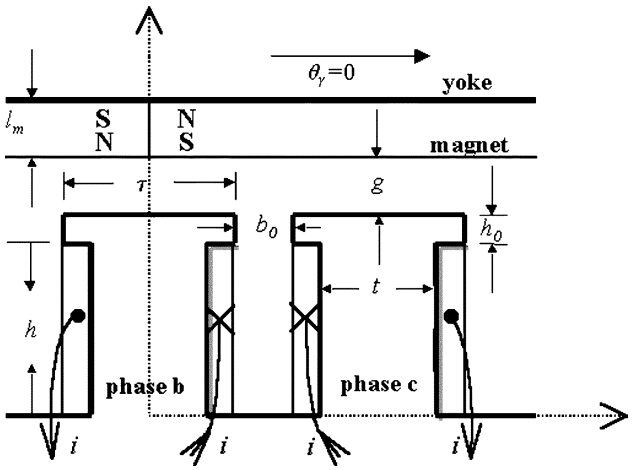

Fig. 1. Simplified shoes, teeth, and slots structure.

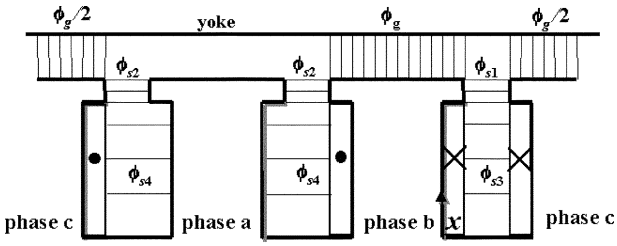

Fig. 2. Flux pattern of winding current.

Thus, this paper is concerned with only $L_{\rm eq}$. Some assumptions listed here are made to simplify the analysis.

- A1) The shoes, the teeth and the slots of the stator are simplified to rectangular shapes with the dimensions b_0, τ, h_0, h, t, l_m and g as shown in Fig. 1.
- A2) For the calculation of the air-gap permeance, the field pattern is assumed to be that the flux lines are always orthogonal to the intersection surface of the air-gap and the steel (see Fig. 2).
- A3) The B-H curve of the PM is linear with the constants of the relative permeability μ_r and the remanence B_r.
- A4) The reluctance of the rotor and the stator back iron are usually seen as zero, so that the magnetic field within the motor can be assumed the linear superposition of the PM and the winding current. The nonlinear interaction of these two fields is considered only for the calculation of the air-gap inductance. This means that the relative permeability μ_{Fe} of the stator back iron is still regarded as a nonlinear function of the flux density in the shoes and the teeth of the stator.

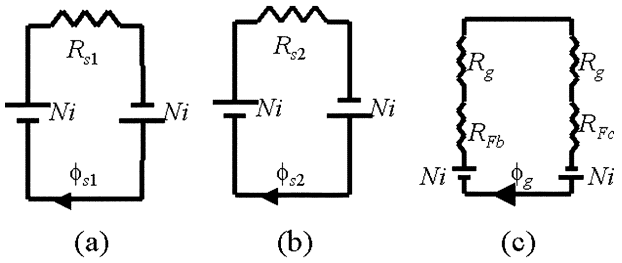

Fig. 3. (a) Equivalent magnetic circuit of ϕ_{s1}. (b) Equivalent magnetic circuit of ϕ_{s2}. (c) Equivalent magnetic circuit of air-gap flux.

Suppose that only two of the three phases are excited by the same winding current i. These two phases are phases b and c in Fig. 1. It is known [5] that $L_{\rm eq}$ is the sum of the air-gap (L_g) and the slot (L_s) inductances

$$L_{\rm eq} = \frac{(L_g + L_s)N_s}{3} \tag{1}$$

where N_s are the total numbers of slots, the divider 3 is the number of the phases of a PMSM. The inductances L_g and L_s are functions of the flux linkage ϕ_g and ϕ_s, respectively. The flux linkages of the windings are shown in Fig. 2, where they are divided into five parts: ϕ_g, ϕ_{s1}, ϕ_{s2}, ϕ_{s3}, and ϕ_{s4}. ϕ_g is the flux crossing the air-gap, while ϕ_s consists of ϕ_{s1}, ϕ_{s2}, ϕ_{s3}, and ϕ_{s4}. Since there is no current in phase a, the flux linkages ϕ_{s2} and ϕ_{s4} cross the shoes and the teeth of phase a, respectively. Thus, L_s can also be divided into four parts as

$$L_s = L_{s1} + L_{s2} + L_{s3} + L_{s4}. \tag{2}$$

The equivalent magnet circuits of ϕ_{s1} and ϕ_{s2} are, respectively, shown in Fig. 3(a) and 3(b). Note that N is the number of turns of each stator tooth, R_{s1} is the magnetic reluctance of ϕ_{s1}, and R_{s2} is that of ϕ_{s2}. It follows from Fig. 3 that $\phi_{s1} = 2Ni/R_{s1}$ and $\phi_{s2} = 2Ni/R_{s2}$. According to the definition of the inductance [6], we obtain

$$L_{s1} = \frac{2N\phi_{s1}}{i} = \frac{4N^2}{R_{s1}} \quad L_{s2} = \frac{2N\phi_{s2}}{i} = \frac{4N^2}{R_{s2}}. \tag{3}$$

It is well known that $R_{s1} = R_{s2}/2 = b_0/(\mu_0 h_0 z)$, where b_0 and h_0 are defined in Fig. 1, z is the motor axial active length, and μ_0 is the permeability of the air. Consider the rectangular slot of flux linkage ϕ_{s3}, in Fig. 2, i.e., the slot between the teeth of phases b and c. The magnetic motive force (MMF) at the top of the slot is equal to $2Ni$, while it is zero at the bottom. This is because the turns are uniformly distributed in the slot, and the magnetic field $H(x)$ crossing the slot increases linearly from the bottom of the slot to the top. Since $H(0) = 0$ and $H(h) = 2Ni/(b_0 + \tau - t)$, we have $H(x) = 2Nix/[(b_0 + \tau - t)h]$, where x is the distance from the bottom of the slot (see Fig. 2). This allows us to express L_{s3} from the energy viewpoint [7] as

$$L_{s3} = \frac{\int_{\rm vol} \mu_0 H^2 dV}{i^2} = \frac{4}{3}\frac{\mu_0 N^2 hz}{(b_0 + \tau - t)} \tag{4}$$

where the integral volume is over the slot volume between phases b and c, i.e., $dV = z(b_0 + \tau - t)dx$. Similarly, L_{s4} can be related to

$$L_{s4} = \frac{2}{3}\frac{\mu_0 N^2 hz}{(b_0 + \tau - t)} = \frac{L_{s3}}{2}. \tag{5}$$

The equivalent magnetic circuit in Fig. 3(c) describes the air-gap flux ϕ_g that goes from the shoe of phase b through the PM yoke to the shoe of phase c and then comes back to the tooth of phase b from the tooth of phase c (see Fig. 2). According to assumption A4), in addition to the reluctance of R_g, only the reluctance of the stator back irons of phases b and c are taken into account, which are denoted by R_{Fb} and R_{Fc}, respectively. R_g, R_{Fb}, and R_{Fc} can be approximated as

$$\begin{cases} R_g = \dfrac{l_m}{\mu_r \mu_0 \tau z} + \dfrac{g}{\mu_0 \tau z} \\ R_{Fb} = \dfrac{h_0}{\mu_0 \mu_{b1} \tau z} + \dfrac{h}{\mu_0 \mu_{b2} t z} \\ R_{Fc} = \dfrac{h_0}{\mu_0 \mu_{c1} \tau z} + \dfrac{h}{\mu_0 \mu_{c2} t z} \end{cases} \tag{6}$$

where l_m, g, τ, h, t, and h_0 are defined in Fig. 1, μ_{b1} and μ_{b2} are the relative permeability of phase b in the shoe and the tooth, respectively, and, μ_{c1} and μ_{c2} are those of phase c. It then follows from Fig. 3(c) that $\phi_g = 2Ni/(2R_g + R_{Fb} + R_{Fc})$. Thus

$$L_g = \frac{2N\phi_g}{i} = \frac{4N^2}{2R_g + R_{Fb} + R_{Fc}}. \tag{7}$$

However, the relative permeability of the stator back iron μ_{b1}, μ_{b2}, μ_{c1} and μ_{c2} are nonlinear functions of the flux densities in the shoes and the teeth of the stator by assumption A4), i.e., $\mu_{b1}(B_{b1})$, $\mu_{b2}(B_{b2})$, $\mu_{c1}(B_{c1})$, and $\mu_{c2}(B_{c2})$ are nonlinear functions, where B_{b1} and B_{b2} are the flux densities of phase b in the shoes and the teeth, respectively, and B_{c1} and B_{c2} are those of phase c. These flux densities are defined as follows:

$$\begin{cases} B_{b1} = \frac{(\phi_{mb} + \phi_g + \phi_{sb})}{\tau z} & B_{b2} = \frac{(\phi_{mb} + \phi_g + \phi_{sb})}{tz} \\ B_{c1} = \frac{(\phi_{mc} - \phi_g + \phi_{sc})}{\tau z} & B_{c2} = \frac{(\phi_{mc} - \phi_g + \phi_{sc})}{tz} \end{cases} \tag{8}$$

where ϕ_{mb} and ϕ_{mc} are, respectively, the fluxes of the PM flowing through phases b and c, and ϕ_{sb}, and ϕ_{sc} are, respectively, the equivalent slot linkage fluxes of phase b and c. ϕ_{mb}, ϕ_{mc}, ϕ_{sb} and ϕ_{sc} can be calculated in advance, but the method for ϕ_{mb} and ϕ_{mc} is complicated and will be described later at the end of this section. It is easy to calculate ϕ_{sb} and ϕ_{sc} with the following equations [6]:

$$\phi_{sb} = \frac{L_s i}{2N} \quad \phi_{sc} = -\frac{L_s i}{2N}. \tag{9}$$

Note that $\phi_{sc} = -\phi_{sb}$, since phases b and c are in series as shown in Fig. 1. It is apparent that B_{b1}, B_{b2}, B_{c1} and B_{c2} are functions of ϕ_g, so that the flux ϕ_g should make the following error function $E(\phi_g)$ zero from the equivalent circuit shown in Fig. 3(c):

$$\begin{aligned} E(\phi_g) &= 2Ni - \phi_g(2R_g + R_{Fb} + R_{Fc}) \\ &= 2Ni - \phi_g \\ &\quad \times \left[\frac{2l_m}{\mu_r \mu_0 \tau z} + \frac{2g}{\mu_0 \tau z} + \frac{h_0}{\mu_0 \mu_{b1}(B_{b1}) \tau z} \right. \\ &\quad + \frac{h}{\mu_0 \mu_{b2}(B_{b2}) t z} + \frac{h_0}{\mu_0 \mu_{c1}(B_{c1}) \tau z} \\ &\quad \left. + \frac{h}{\mu_0 \mu_{c2}(B_{c2}) t z}\right] \\ &= 0. \end{aligned} \tag{10}$$

$E(\phi_g)$ in (10) is a nonlinear equation with a single variable ϕ_g. Applying the Newton–Raphson iteration method to (10), we can easily obtain ϕ_g that makes $E(\phi_g) \approx 0$, provided that ϕ_{mb} and ϕ_{mc} are known. After ϕ_g is obtained, L_g can be calculated

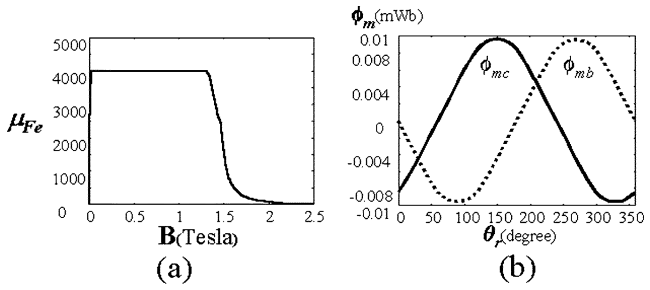

Fig. 4. (a) B $-$ μ_{Fe} curve of the stator back iron. (b) ϕ_{mb} and ϕ_{mc} with respect to θ_r.

by (7). ϕ_{mb} is the PM flux flowing through the coils of phase b and is in the form of

$$\phi_{mb} = z \int_l B_{mg} dl \tag{11}$$

where B_{mg} is the PM flux density in the air-gap, and the integral path l is along the edges of stator shoes of phase b, i.e., the length of the path l is $h_0 + \tau + h_0$ (see Fig. 1). B_{mg} is a function of revolution angle θ_r, and can be predicted by a conventional 2-D analytical method [8]. ϕ_{mc} can be obtained in a similar method.

III. Example

A 3-phase, 12-pole, and 9-slot dc brushless motor used as a spindle motor of a 50x CD-ROM is taken as an example. The motor has a Y-connected windings, surface-mounted NdFeB magnets with $B_r = 0.685$ T and $\mu_r = 1.29$, and nonlinear iron steels with the B $-$ μ_{Fe} curve as shown in Fig. 4(a), where μ_{Fe} is the relative permeability of the stator iron. It shows that the stator iron will be saturated when B, magnetic flux density, is about 1.3 T. The geometrical parameters of the motor are $b_0 = 1.14$ mm, $\tau = 5.67$ mm, $h_0 = 1.35$ mm, $h = 3.55$ mm, $l_m = 1.15$ mm, $t = 1.4$ mm, $z = 4.9$ mm, $g = 0.3$ mm, and $N = 34$.

It is assumed that only two phases b and c are excited by the same current i as shown in Fig. 1. It is revealed in (7) that L_g is proportional to ϕ_g/i, and ϕ_g is a nonlinear function of i, so L_g varies with i. In the example, L_g of the motor is computed for several current levels ($i = \pm 0.2$ A, ± 0.4 A, ± 0.6 A, ± 0.8 A, and ± 1 A) and different rotor positions θ_r over the entire 360° electrical cycle.

We can calculate out the slot inductances, $L_{s1} = 33.7$ μH, $L_{s2} = 16.9$ μH, $L_{s3} = 6.2$ μH, and $L_{s4} = 3.1$ μH from (3)–(5), respectively. The total slot inductance is then $L_s = 60$ μH by (2). Furthermore, we use (9) to obtain $\phi_{sb} = 0.88i$ μWb and $\phi_{sc} = -0.88i$ μWb. They are both proportional to i. Note that ϕ_{mb} and ϕ_{mc} are functions of θ_r, and are calculated using (11). The results of them are shown in Fig. 4(b). Substituting ϕ_{sb}, ϕ_{sc}, ϕ_{mb}, and ϕ_{mc} into (8), we obtain B_{b1}, B_{b2}, B_{c1}, and B_{c2}, and then $\mu_{b1}(B_{b1})$, $\mu_{b2}(B_{b2})$, $\mu_{c1}(B_{c1})$, and $\mu_{c2}(B_{c2})$ from Fig. 4. Note that ϕ_{mb} and ϕ_{mc} vary with the rotor position θ_r, so do $\mu_{b1}(B_{b1})$, $\mu_{b2}(B_{b2})$, $\mu_{c1}(B_{c1})$, and $\mu_{c2}(B_{c2})$. Finally, ϕ_g is calculated out by solving $E(\phi_g) = 0$ in (10) with the Newton–Raphson method. It then allows us to compute L_g by (7) and $L_{\rm eq}$ by (1) for several distinct exciting currents i and different θ_r. The results

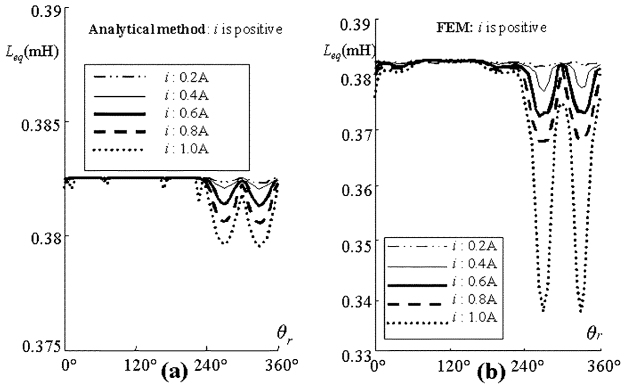

Fig. 5. Results of $L_{\rm eq}$. (a) Proposed analytical method. (b) An FEM.

of $L_{\rm eq}$ are shown in Fig. 5(a). The counterpart results of $L_{\rm eq}$ obtained by a FEM is also shown in Fig. 5(b). The profile of $L_{\rm eq}$ for negative currents is the same but with the 180° phase shift, so is not shown in the paper.

The results of both methods are consistent except that the W shapes in the FEM have larger depths. The possible reason for this difference is that the assumption A4) used to develop (3)–(5) ignores the perturbation of the PM fluxes for the slot inductance. The slot inductance may diminish rapidly in the same way as the air-gap inductance, as the flux density of the iron reaches the saturation state. However, the analytical method does not consider this effect.

IV. Conclusion

This paper proposes an analytical method to calculate the incremental inductance of a PMSM, which is computationally much more efficient than FEM. An example is used to illustrate the proposed analytical method. The results of the analytical method is found very close to those of a FEM with the exception of the difference in the lower peak values of the incremental inductance. Fortunately, this difference does not affect the usefulness of the proposed method.

References

[1] Z. Q. Zhu, D. Howe, and J. K. Mitchell, "Magnetic field analysis and inductances of brushless DC machines with surface-mounted magnets and nonoverlapping stator windings," *IEEE Trans. Magn.*, vol. 31, pp. 2115–2118, May 1995.

[2] D. A. Lowther and P. P. Silvester, *Computer-Aided Design in Magnetics*. New York: Springer-Verlag, 1986.

[3] N. A. Demerdash, F. A. Fouad, and T. W. Nehl, "Determination of winding inductances in ferrite type permanent magnet electric machinery by Finite Elements," *IEEE Trans. Magn.*, vol. MAG-18, pp. 1052–1054, Nov. 1982.

[4] M. Gyimesi and D. Ostergaard, "Inductance computation by Incremental Finite Element analysis," *IEEE Trans. Magn.*, vol. 35, pp. 1119–1122, May 1999.

[5] T. J. E. Miller, M. I. Mcgilp, D. A. Staton, and J. J. Bremner, "Calculation of inductance in permanent-magnet DC motors," *Proc. Inst. Elect. Eng.—Elect. Power Applicat.*, vol. 146, no. 2, pp. 129–137, 1999.

[6] F. W. Sears and M. W. Zemansky, *University Physics*. Reading, MA: Addison-Wesley, 1979.

[7] D. C. Hanselman, *Brushless Permanent Magnet Motor Design*. New York: McGraw-Hill, 1993.

[8] Z. Q. Zhu and D. Howe, "Analytical prediction of the cogging torque in radial-field permanent magnet brushless motors," *IEEE Trans. Magn.*, vol. 28, pp. 1371–1374, Mar. 1992.